Energy Equip. Sys./ Vol. 10/No. 3/Sep. 2022/ 271-286

ENERGY EQUIPSYS

Energy Equipment and Systems

http://energyequipsys.ut.ac.ir
www.energyequipsys.com

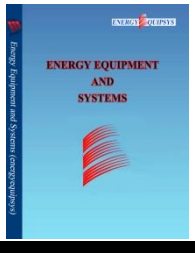

Fault detection and isolation of wind turbine gearbox via noise-assisted multivariate empirical mode decomposition algorithm

Authors

Shahin Siahpour[a]
Moosa Ayati[b]*
Mohamadreza Haeri-Yazdi[b]
Mohammad Mousavi[c]

[a] Department of Mechanical and Materials Engineering, University of Cincinnati, Cincinnati, OH, USA

[b] School of Mechanical Engineering, College of Engineering, University of Tehran, Tehran, Iran

[c] Department of Mechanical Engineering, State University of New York at Binghamton, Binghamton, NY, USA

Article history:

Received : 16 May 2020
Accepted : 28 April 2021

ABSTRACT

The wind turbine power transmission system exploits a planetary gearbox due to its large power transmission. In comparison with the common rotating systems, the wind turbine (WT) gearbox is assumed a complex system. Therefore, condition monitoring and fault detection isolation (FDI) of such systems are not straightforward and conventional signal processing methods (e.g. Fast Fourier transform) are not applicable or do not have an acceptable output accuracy. This paper proposes a new FDI approach for wind turbines based on vibration signals' signatures derived from the multivariate empirical mode decomposition (MEMD) algorithm. Vibration signals are measured from a 750 kW planetary wind turbine gearbox on a dynamometer test rig provided by National Renewable Energy Laboratory (NREL). In WT applications, to gather enough data with high accuracy and to avoid losing local information, multiple sensors must be utilized to collect data from different locations of the gearbox yielding a multi-sensory dataset. In standard EMD, joint information of multi-sensory data will be lost. Additionally, the intrinsic mode function (IMF) groups may not have the same characteristic features. To capture cross information of the dataset and to remove the effect of noise on the output results, a noise-assisted MEMD (NA-MEMD) algorithm is employed. Vibration signal features are also extracted by using discrete wavelet transform (DWT). Three major faults of the WT gearbox are detected using NA-MEMD and a comparison between NA-MEMD and DWT methods confirms the capability of the NA-MEMD method.

Keywords: Multivariate Empirical Mode Decomposition (MEMD), Noise-Assisted MEMD, Vibration Signals Signature, Wind Turbine Gearbox, Fault Detection and Isolation.

1. Introduction

Planetary gearboxes are widely used in mechanical transmission systems such as wind turbine drivetrains due to the large power transmission in a compact structure. Wind turbines are working in harsh conditions and random behaviors of the wind speed which may lead to failure and shutdown of the entire system [1]. Gearbox subsystem faults and failures are

*corresponding author: Moosa Ayati
School of Mechanical Engineering, College of Engineering, University of Tehran, Tehran, Iran
Email: m.ayati@ut.ac.ir

the most frequent amongst wind turbine mechanical subsystems [2]. In many cases, without a proper maintenance system, the wind turbine would fail in almost five years while the wind turbine's average design life is 20 years [3]. Thus, powerful condition monitoring (CM) or FDI systems is vital for the safe and efficient operation of WT during its lifetime.

There are many ways for FDI of wind turbine gearboxes, such as vibration analysis, acoustic emission, ultrasonic testing techniques, oil analysis and thermography [4]. Among these methods, vibration analysis is a commonly used approach for condition monitoring. The basic idea is that rotating machinery has specific vibration signatures and these signatures change when there is a fault in some parts of the machinery. In early studies, some of the conventional techniques such as skewness and kurtosis [3] or Cepstrum analysis [5] were used to extract fault features from the systems. These methods are mostly used when the system is operating at a constant speed [6]. Complex systems such as the wind turbine gearbox cannot be analyzed with these methods. Instead, more advantageous condition monitoring techniques such as short-time Fourier transform [7], wavelet transform [8], empirical mode decomposition (EMD)[9], and Hilbert-Huang transform [10] should be utilized.

In wavelet transform, to determine wavelet coefficient, some wavelet bases are required to be chosen where results of the analysis are influenced by the choice of these bases. On the other hand, EMD is a self-adaptive nonlinear and nonstationary data analysis technique and does not require basis functions for analyzing signals. In the EMD algorithm, oscillatory modes work as the basis function and they are determined by raw signal rather than by pre-defined functions. Thus, EMD is widely applicable in fault detection of systems and machinery[11,12]. Fang and Ming [13] investigated the EMD algorithm for fault detection of gearbox and exploited Hilbert transform to determine instantaneous frequencies. EMD algorithm decomposes nonlinear and nonstationary signals into some almost orthogonal and stationary time series representations of the signal, which are called intrinsic mode functions (IMFs) of the signal [14]. In order to prevent the mode mixing phenomenon for noisy signals, ensemble empirical mode decomposition (EEMD) can be employed[9,15].

Usually, in complex systems such as wind turbine gearbox, to obtain data more precisely instead of using one sensor, several sensors are used and placed in different locations of the system, yielding a multivariate signal. When dealing with multivariate signals by standard EMD algorithm, each signal is processed individually [16]. Extracting fault features from individual IMF groups causes some problems in the fault detection procedure. For instance, there is the possibility that decomposition results from different sensors do not match in frequency content or number of IMFs[17]. Another problem is that when each signal is treated individually, results cannot show the correlation information between signals[18].

To cover the limitation of the standard EMD algorithm with multivariate signals, Rilling et al. proposed a bivariate EMD algorithm in 2007 [19]. In this method, the local mean is calculated by mapping the bivariate signal in several directions and averaging the local mean of this projected signal. Tsoumas et al. [20] used this method to analyze the bivariate vibration signal of a rotor. Pursuing the bivariate idea, in 2010 Rehman and Mandic [21] proposed trivariate EMD to deal with three-dimensional signals. This idea is generalized to multivariate EMD by Rehman [22] for n-dimensional signals. Multivariate EMD allows the processing of the n-dimensional signal (obtained from sensors located in different positions), simultaneously. MEMD solved the problems of processing each signal individually. Multivariate signals from multiple sensors provide joint information applicable in condition monitoring and fault detection of rotating machines [23] and bearings [18]. In the same situation as the univariate signal analysis, the mode mixing phenomenon is almost inevitable in the MEMD algorithm if the input signals are noisy. Noise-assisted MEMD (NA-MEMD) is proposed to eliminate the interference of noise in the MEMD algorithm [24].

In this paper, a novel fault detection and isolation procedure is proposed for extracting fault features from the wind turbine gearbox. NA-MEMD algorithm is used to extract fault features from the studied wind turbine gearbox.

Vibration signals are from a 750 kW planetary wind turbine gearbox on a dynamometer test rig provided by National Renewable Energy Laboratory (NREL). Since eight sensors are exploited for gathering vibration data, MEMD reveals its advantage over standard EMD. Besides the complexity of the system, three faults, i.e. High-speed stage, planetary stage, and high-speed stage bearings, are present in this system. Apart from fault signatures that exist in faulty signals in special frequencies, there are other features in the healthy signals related to the system dynamics and nature. Therefore, first, healthy signal characteristics are investigated and then compared with the faulty signal. To show the strength of the MEMD algorithm, fault features are also extracted by discrete wavelet transform (DWT) [25] and this comparison is made by a newly defined amplitude factor.

The paper is organized as follows. Section 2 explains the mathematics of the standard EMD algorithm and multivariate EMD. Section 3 introduces the wind turbine gearbox that is used for this study and shows some mechanical characteristics (e.g. meshing frequency) and explains how vibration signals are measured and prepared. Section 4 presents the numerical results by applying the proposed FDI approach to the vibration signals of the gearbox. The conclusion is given in Section 5.

2. Background of EMD

2.1. Fundamentals of the EMD algorithm

This method is firstly introduced by Huang et al. [26]. The basic idea of this method is that every signal consists of some intrinsic mode functions (IMF). Each of these IMFs must satisfy two conditions: (1) on the entire length of the IMFs, number of extrema and zero-crossings must be either equal or at most differ by one, and (2) at any point, the mean value of the envelope defined by local maxima and the envelope defined by the local minima is zero. The following steps are the process for obtaining IMFs of a signal which is called the *sifting process* [27].

1. Find upper envelope $u(t)$ and lower envelope $l(t)$ of signal $x(t)$ by connecting all the local maxima and the local minima, respectively. This connection is usually made as cubic spline interpolation of the extrema.
2. Compute the average of the upper and lower envelope, $m(t)$ which is called envelope mean using

$$m(t)=\frac{u(t)+l(t)}{2} \tag{1}$$

3. Compute $h(t)=x(t)-m(t)$ called "oscillatory mode".
4. Choose $h(t)$ as IMF only if it satisfies the previously mentioned conditions of IMFs, or else treat $h(t)$ as the signal $x(t)$ and repeat steps 1 to 3. This process must be done until $h(t)$ satisfies IMF conditions. Then, name this IMF by $c_1(t)$.
5. Subtract the IMF from the signal $x(t)$ which results in the residual signal $r_1(t)$:

$$r_1(t)=x(t)-c_1(t) \tag{2}$$

$r_1(t)$ denotes residual signal related to the first IMF. $r_1(t)$ must be used as a new dataset signal and the sifting process must be repeated in a way that each residual signal for the ith IMF, i.e. $r_i(t)$, is used as a new dataset signal for subsequent steps until the residual signal $r_N(t)$ become a monotonic function. The IMF's $\{c_i(t)\}_{i=1}^{N}$ include different frequency bands ranging from high to low. The original signal is reconstructed as the summation given by

$$x(t)=\sum_{i=1}^{N}c_i(t)+r_N(t) \tag{3}$$

2.2. Multivariate EMD

Standard EMD calculates the local mean by averaging the upper and lower envelopes. These envelopes are obtained by interpolation of local maxima and minima. However, for multivariate signals, the value of local maxima and minima cannot be directly defined and this makes it rather confusing to determine IMF defined by oscillatory modes. To overcome these problems, multivariate EMD is developed. According to this method, n-variate signal is regarded as n-dimensional time series. Each signal is projected on an appropriately selected direction and multidimensional envelopes (which will explain in a subsequent paragraph) are generated afterward. Then, the average of

these envelopes is taken as a local mean of the envelopes. After this process to calculate the IMFs, previously explained steps 3 to 5 (in section 2.1) are used.

The accuracy of the calculation of the local mean with this method depends on how uniformly the direction vectors are chosen. The direction vector in n-dimensional space can be considered as points on the unit $(n-1)$ dimensional sphere. There are two main methods for achieving the uniform sampling point sets in the multivariate EMD [22]: (1) Uniform angular sampling. In this method, uniform angular sampling of a unit sphere in an n-dimensional sphere coordinates for a set of direction vectors is employed. The resulting set of direction vectors spans the whole sphere. Although this method makes an easy way to generate point sets, it cannot provide a completely uniform distribution for $n > 1$, because there is a higher density of points at the poles of the sphere. (2) A Quasi-Monte Carlo-based sampling based on low-discrepancy point sets (family of Halton and Hammersley sequences). Halton and Hammersley are used in this paper and are introduced as an example of the quasi-Monte Carlo lower deviation sequence.

let $x_1, \dots, x_n$ be the first n prime numbers and ith sample of a one-dimensional Halton sequence, denoted by r_i^x, is given by

$$r_i^x = \frac{a_0}{x} + \frac{a_1}{x^2} + \dots + \frac{a_s}{x^{s+1}} \tag{4}$$

where the base-x representation of i given by

$$i = a_0 + a_1 x + \dots + a_s x^s \ . \tag{5}$$

Starting from $i = 0$, the i sample of the Halton sequence then becomes

$$\left(r_i^{x_1}, r_i^{x_2}, \dots, r_i^{x_n}\right). \tag{6}$$

The Hammersley sequence is used when the total number of samples, n, is known *a priori*; in this case, the i sample within the Hammersley sequence is calculated as

$$\left(i/n, r_i^{x_1}, r_i^{x_2}, \dots, r_i^{x_{n-1}}\right) \tag{7}$$

By using Halton and Hammersley sequences, a suitable set of direction vectors on the n sphere is generated. Henceforth, projections of signals on this direction vectors will be calculated. In the following paragraph multivariate EMD will be explained briefly.

Let $X(t) = [x_1(t), x_2(t), \dots, x_n(t)]$ be a n-dimensional signal and $D^k = \{d_1^k, d_2^k, \dots, d_n^k\}$ correspond to the kth direction vector in a direction set, D. The multivariate EMD algorithm is described as followed:

1. Choose a suitable set of direction vectors, D.
2. Calculate the kth projection, $p^k(t)$ of X along the kth direction where $k = 1,2, \dots, K$, and K is the total number of direction vectors.
3. Find the time instants, t_i^k, corresponding to the maxima of projected signals.
4. Interpolate $\left[t_i^k, X(t_i^k)\right]$ to determine multidimensional envelopes, $E^k(t)$.
5. Calculate the mean by

$$M(t) = \frac{1}{l}\sum_{k=0}^{K} E^k(t). \tag{8}$$

6. Calculate the residual component $R(t) = X(t) - M(t)$. If $D(t)$satisfies the stopping criterion which explains the previous section, then consider $R(t)$ as an IMF then repeat the algorithm until it meets the criterion.

To clarify this MEMD algorithm, Fig. 1 schematically illustrates the flowchart of the multivariate EMD algorithm.

2.3. Noise-assisted multivariate EMD

Whenever the input signal for the MEMD algorithm is noisy, the mode mixing phenomenon is almost inevitable. NA-MEMD algorithm is an extension of the MEMD method to remove the effect of noise in the input signals. The following steps represent the algorithm.

1. Create an *l*-channel of uncorrelated Gaussian white noise time series which have the same length as that of the input ($l \geq 1$).
2. Add noise channels, created in step 1, to the input signals which results in the new input signal with $(n + l)$-channel.
3. Decompose the $(n + l)$-channel multivariate signal using the MEMD algorithm to obtain IMFs.
4. Discard *l* channels corresponding to the noise from $(n + l)$-variate IMFs and get

n-channel IMFs corresponding to the original signal.

3. System Description

In this section, the studied wind turbine gearbox is introduced. The vibration data are provided by the National Renewable Energy Laboratory (NREL). The wind turbine gearbox consists of one low-speed (LS) planetary stage and two parallel stages including intermediate speed and high-speed stages. The test drive is designed for a turbine with a rated power of 750 kW. The Gearbox has an overall ratio of 1:81.491. Figure 2 shows characteristic frequencies schematically.

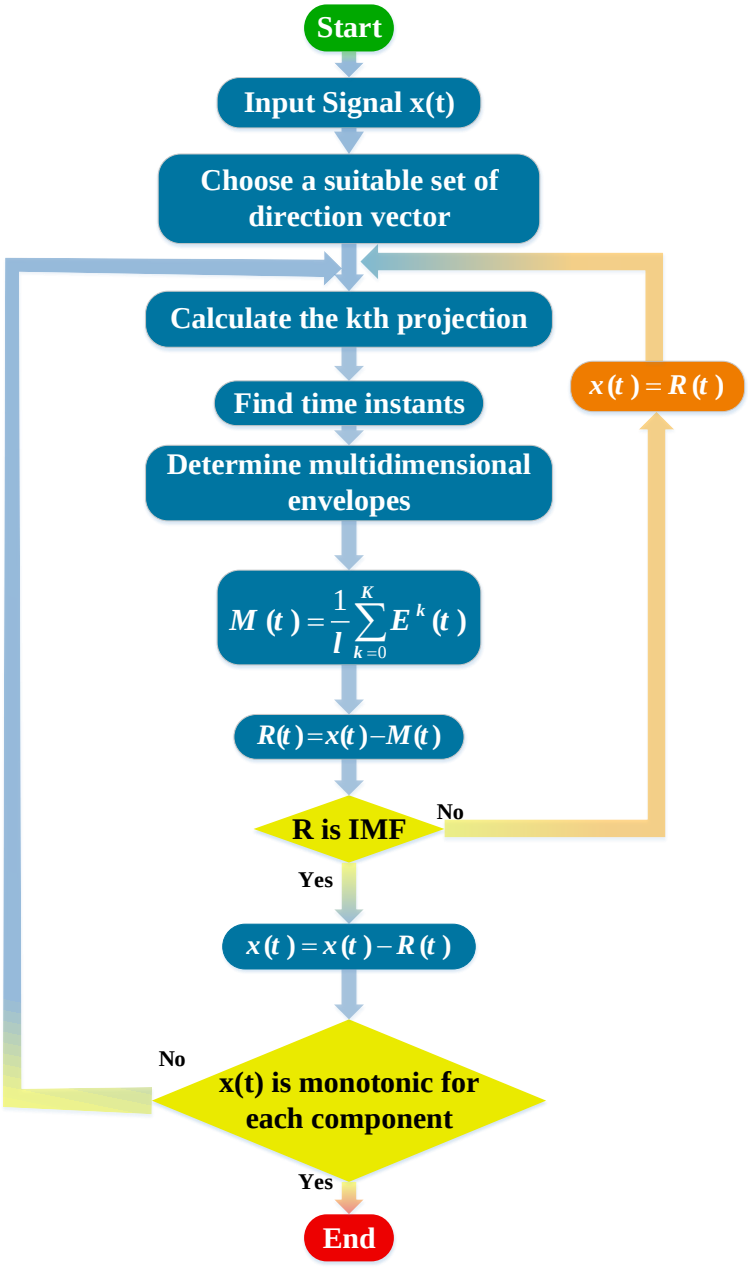

Fig. 1. Multivariate EMD algorithm flowchart

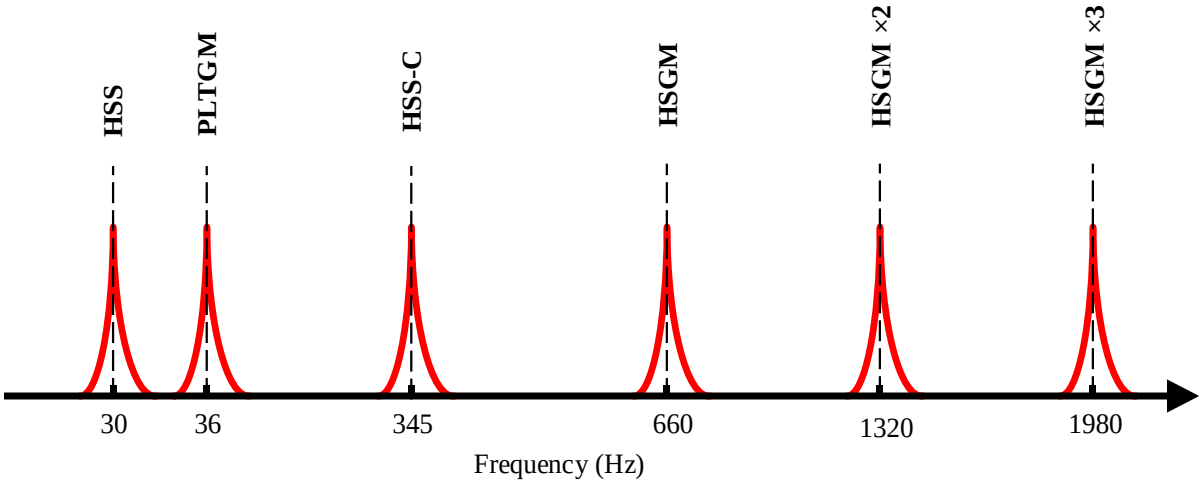

Fig. 2. Characteristic frequencies of the gearbox

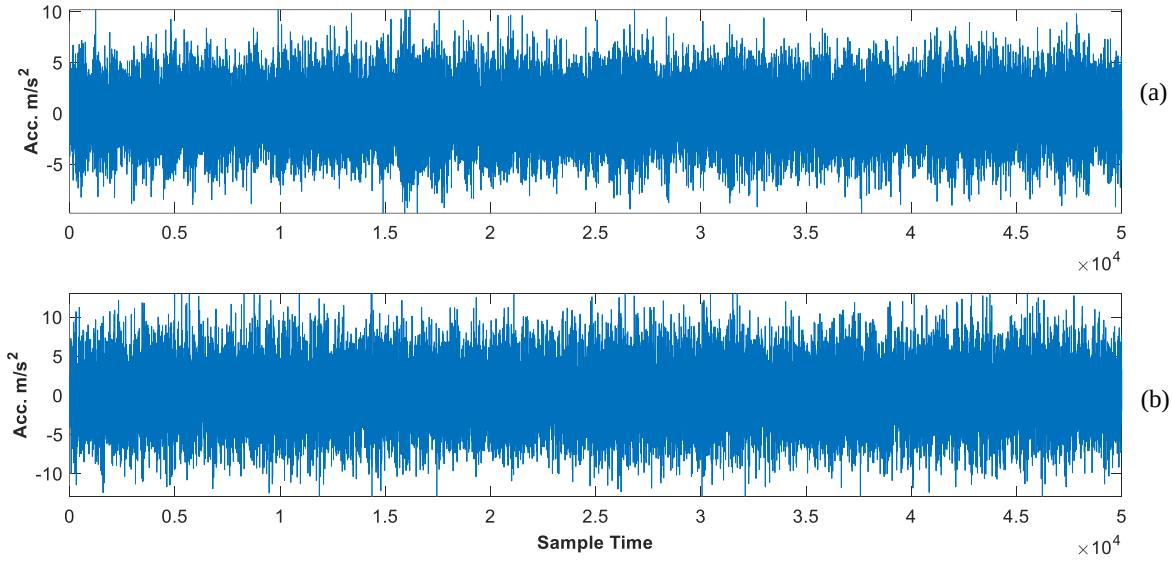

Fig. 3. Time-domain vibration signal from sensor AN7 for (a) healthy (b) faulty condition (50 000 samples are plotted)

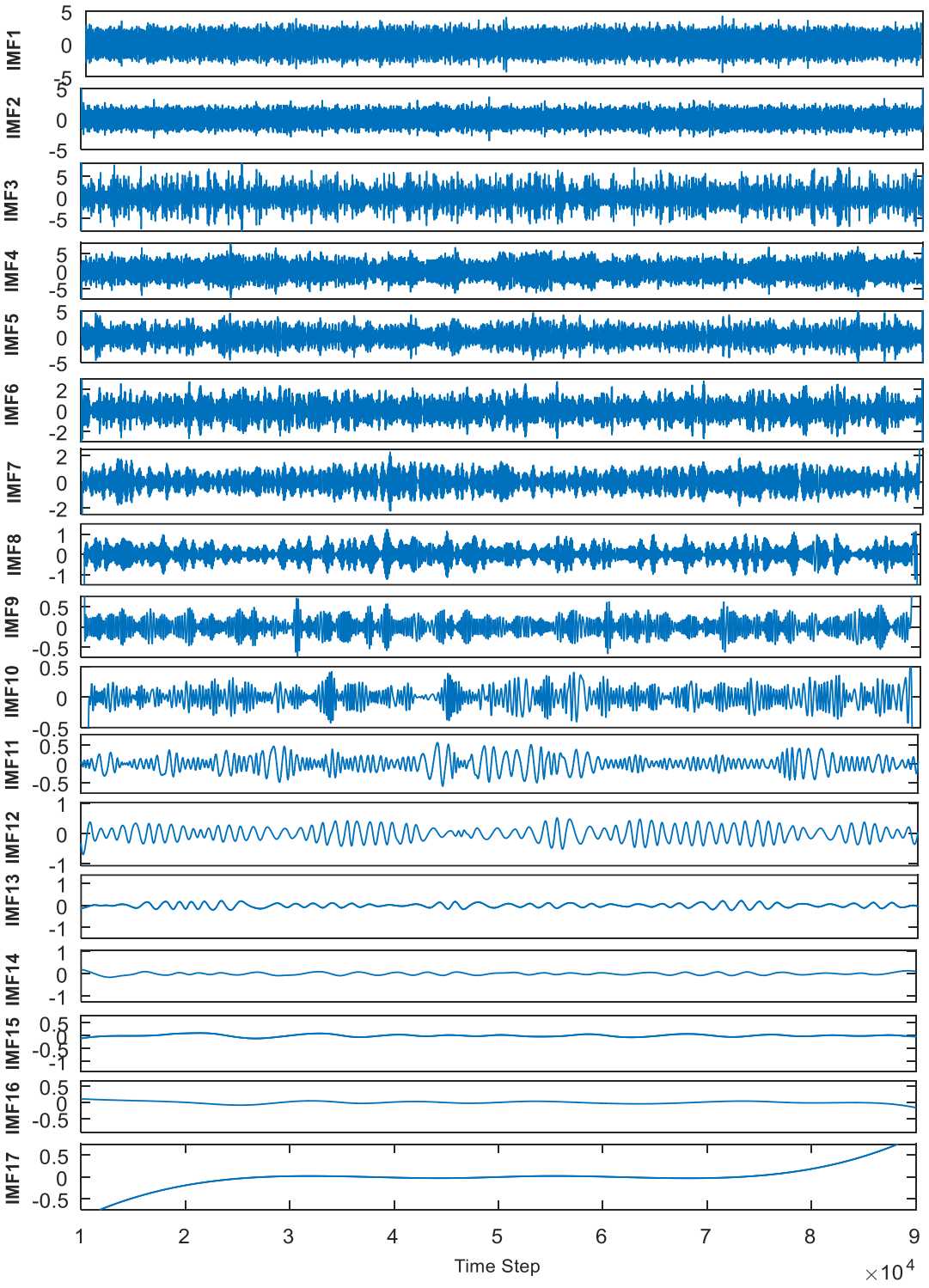

Fig. 4. IMF of the healthy signal of sensor AN7 by MEMD algorithm

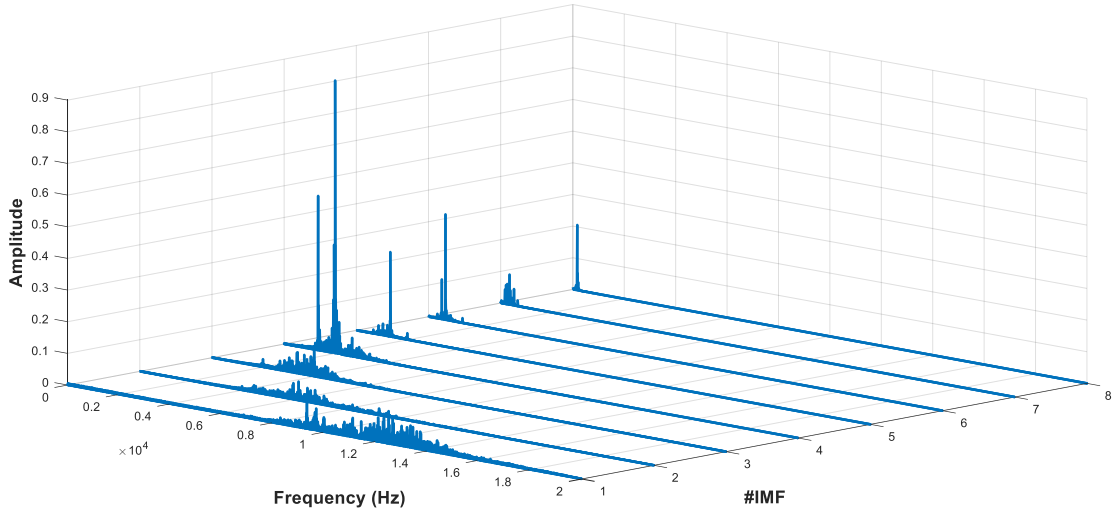

Fig. 5. FFT of first eight IMFs of signal from sensor AN7

4. Experimental results

To implement the NA-MEMD algorithm on the signals, three noise channels are added to the original signals. Noise signals are white Gaussian signals and the corresponding power is -10 dB.

4.1. Healthy condition

To diagnose a fault in the rotary machine, the healthy condition of the system must be studied and identified for the comparison of the faulty condition. Figure 3 shows time-domain vibration data from sensor AN7 for healthy and faulty conditions. The wind turbine gearbox is planetary and its time-domain features are very complicated. As it is seen, finding faults from the time-domain representation of the wind turbine gearbox is not practical.

As was mentioned before, eight sensors collect the vibration data and with the help of these data, multivariate EMD can be exploited. Figure 4 depicts the decomposed healthy signals with the NA-MEMD algorithm for AN7. The last IMF must be a monotonic function which is illustrated in this figure. To evaluate signals and extract features from them, each IMF is investigated in the frequency domain. Figure 5 illustrates the first eight IMFs of the healthy signal of sensor AN7. As it is seen, in some IMFs there are some peaks in some particular frequencies. These frequencies are rotating and meshing frequencies of the wind turbine gearbox. As will be discussed in the following section, faulty signals have these kinds of peaks. To distinguish between healthy and faulty peaks, healthy and faulty signals must be compared with each other.

As was mentioned, in this study in addition to the MEMD algorithm, fault detection using discrete wavelet decomposition is investigated and a comparison between these two methods is conducted. Figure 6 shows the decomposed healthy signal using discrete wavelet transform. Mother wavelet db4 is used [28] for decomposition [25] since it shows the best results in comparison with other groups of mother wavelets.

4.2. Faulty condition

In this section, vibration signals of the wind turbine with faults are investigated, and for a better understanding of vibration signals, a comparison between faulty and healthy signals is done. Also, discrete wavelet decomposition is performed to evaluate the MEMD algorithm in comparison with the well-known WT method for fault detection of rotating machines.

Figure 7 illustrates the 6th IMFs of each signal. As it was mentioned previously, an advantage of multivariate EMD over standard EMD is that each IMF group has similar characteristics. This helps to extract fault features more conveniently and it is an

important characteristic to extract fault features, automatically (e.g. for intelligent fault detection methods). Figure 7 verifies this matter. Since each IMF consists of an almost certain frequency, each IMF is used to extract a specific fault. In the 6th IMF for each signal, there is a peak at gear mesh frequency (661 Hz) and this frequency feature exists in all the same IMF groups for each signal. In contrast to MEMD output results, high-speed shaft fault features fluctuate between the 6th and 7th IMFs that is resulted from the EMD algorithm; therefore, one cannot be sure that a specific fault feature exists in a specific IMF group. In another word, because of the same frequency characteristics, each IMF group can be regarded as a fault feature in the MEMD algorithm which is a privilege over the EMD algorithm.

To this point, the advantages of the MEMD algorithm over EMD are demonstrated. From now on, the capabilities of the MEMD algorithm to extract fault features are investigated. The studied wind turbine gearbox has three major faults. In the subsequent sections, each fault is examined individually.

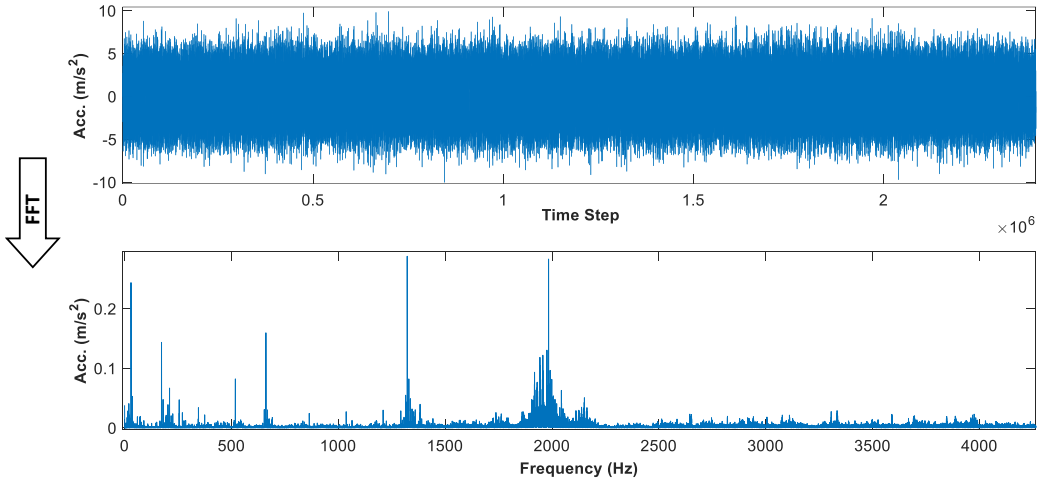

Fig. 6. The second level of approximation of a healthy signal and its FFT

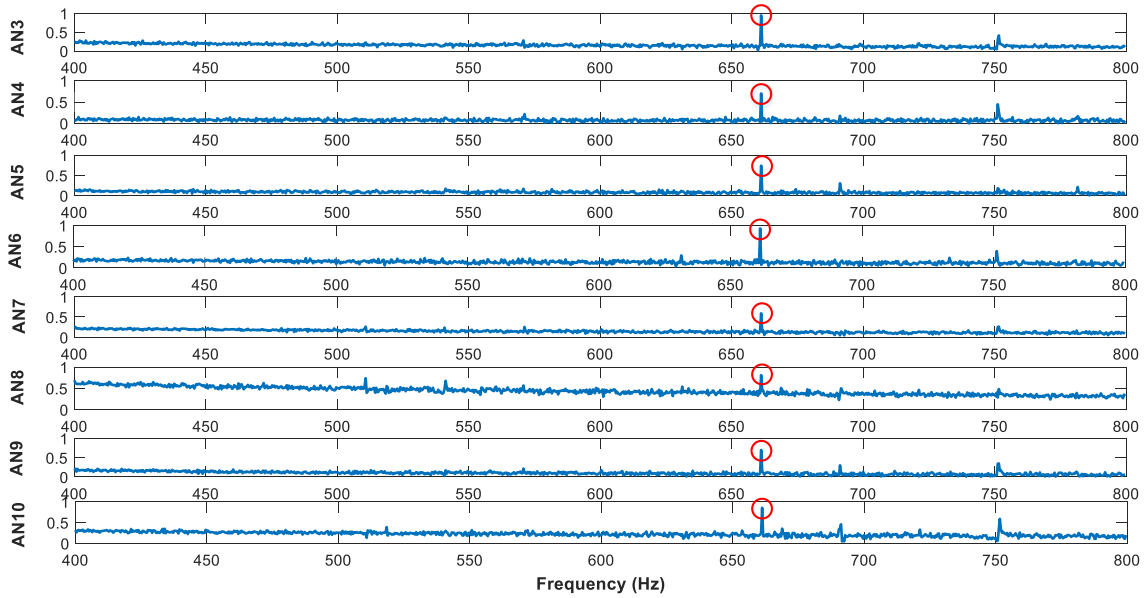

Fig. 7. Comparison of 6th IMF of signals from each sensor

- High-speed stage faults

The most severe fault is in this part of the wind turbine gearbox. The high-speed shaft rotates at 1800 rpm (30 Hz). The high-speed pinion has 22 teeth and the meshing frequency for high-speed gears is $f_{HSGM} = 660$ Hz. Figure 8 demonstrates the comparison between two faulty and healthy decomposed signals using the NA-MEMD algorithm. As is seen from this figure, there is a peak at 661 Hz which is very close to the meshing frequency of a high-speed shaft (f_{HSGM}). The point is that both healthy and faulty IMFs have this peak but the peak for faulty signals IMF has a higher amplitude than the peak of healthy signals IMF. Therefore, it is an indication that there might be a fault in the high-speed shaft gears. By looking closely at the figure, a peak is seen at $f_{HSGM} + f_{HS}$ =691.2 Hz where, $f_{HS} = 30$ Hz is a high-speed shaft frequency.

It can be concluded that the probability of fault existence in high-speed pinion is high. Discrete wavelet decomposition is done to extract high-speed stage fault features. Figure 9 shows a comparison between the healthy and faulty second-level approximation of the AN5 signal. There are peaks at meshing frequency and its harmonics. As it was discussed in the previous paragraph, since there are peaks at meshing frequency and its harmonics and these peak amplitudes are much higher than healthy condition harmonics, it can be concluded that there might be faults in the high-speed stage gears. Sidebands are very distinguishable in this method. These sidebands show which gear in the high-speed stage contains some faults in it. Since the sideband frequency is 30 Hz which is a high-speed shaft frequency, there are faults in the high-speed pinion.

To make the comparison more understandable and more quantitative, a new amplitude factor is introduced to distinguish if a peak in the signal's IMFs presents a fault or not. The factor is the division of the amplitude of the peak at a certain frequency in a faulty signal by the amplitude of the peak at the same frequency in the healthy signal. In Table 1 this factor is calculated for the 6th IMF of all the eight sensors' signals. According to this table, amplitude factors for wavelet coefficient are higher than IMFs which means that high-speed stage faults are more distinguishable by using discrete wavelet transform decomposition. However, an important point must be considered. IMFs contain almost a certain frequency. In other words, each IMF has one distinguishable peak and this makes it more convenient to detect fault by MEMD. To determine the location of fault more precisely, sidebands are helpful and these sidebands are more recognizable by wavelet coefficients.

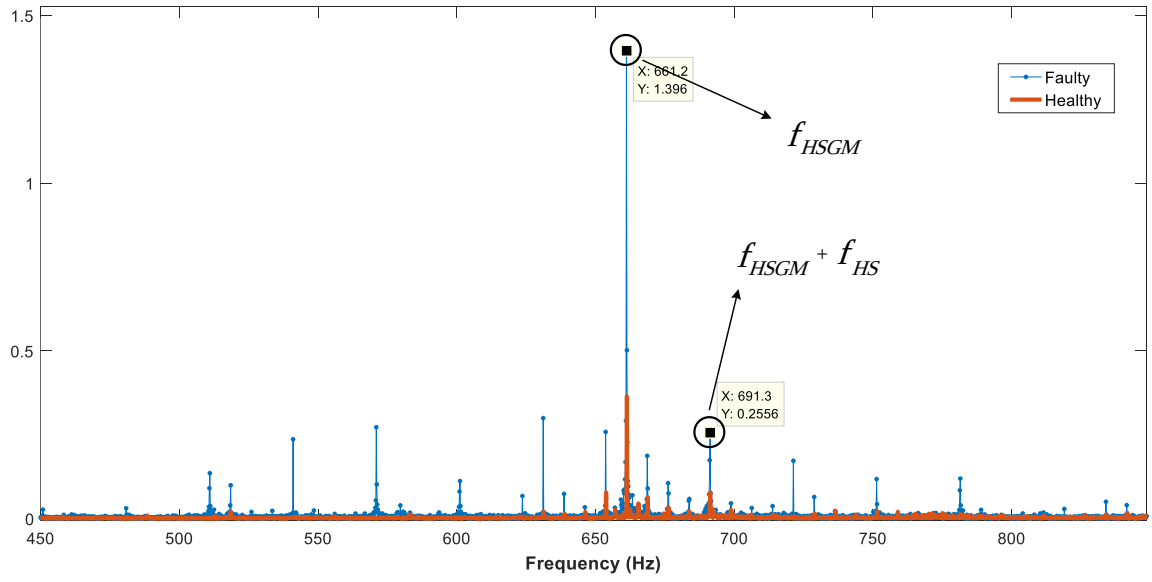

Fig. 8. Comparison between 6th IMF of AN5 sensor for healthy and faulty conditions

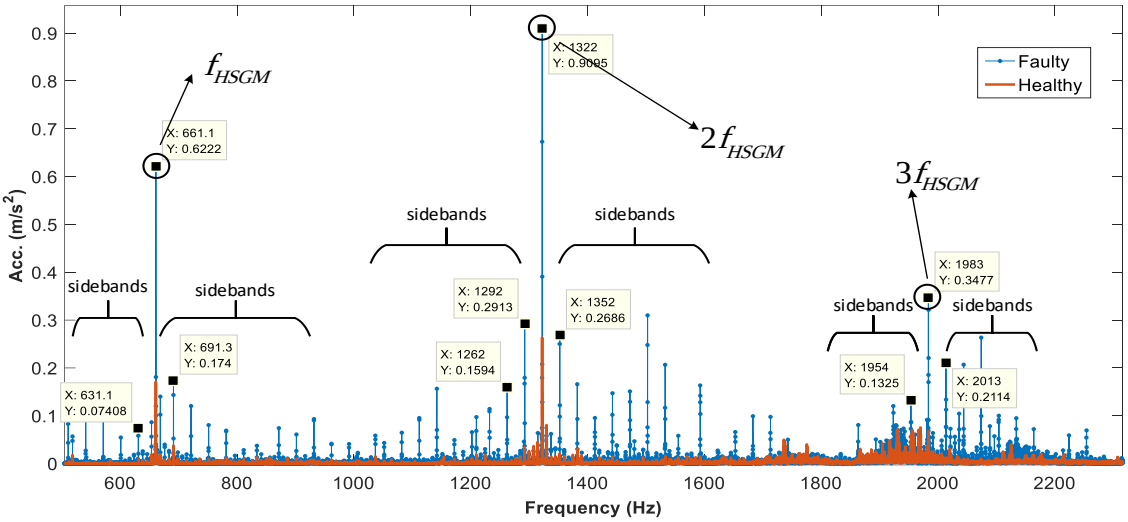

Fig. 9. FFT of the second level of discrete wavelet decomposition of healthy and faulty signals of AN5 sensor

- Planetary stage faults

There is another fault in the planetary stage which is investigated in this section. The meshing frequency of the planetary gearbox is $f_{PLTGM} = 36.4$ Hz. A comparison between the 12th IMFs of healthy and faulty signals from sensor AN3 is illustrated in Fig. 10. As it is obvious in this figure, there is a peak both in healthy and faulty IMFs. This peak is at the high-speed shaft frequency and is another sign of the existence of faults in the high-speed stage. There is a peak at planetary meshing frequency in the faulty IMF which has a higher amplitude than a healthy signal. This indicates that there might be faults in the planetary stage of the gearbox system. The post-test examination confirmed that there are scuffing and polishing damages in the ring gear [29].

Table 1. Amplitude factor for 6th IMF of signals and second level DWT coefficient

	Signal 1	Signal 2	Signal 3	Signal 4	Signal 5	Signal 6	Signal 7	Signal 8
NA-MEMD	3.34	2.96	3.11	3.42	2.76	3.06	2.87	3.25
DWT	4.33	3.98	4.17	4.36	3.68	4.28	3.88	4.04

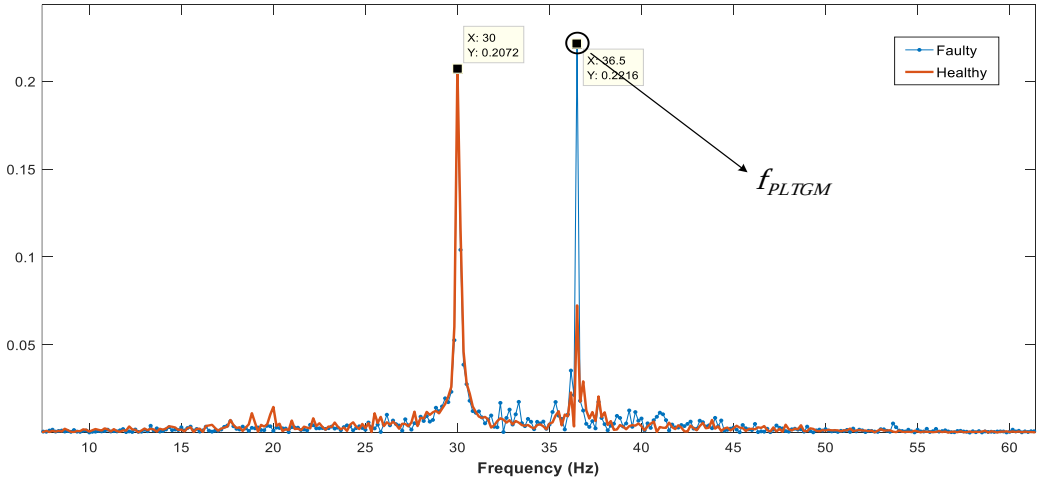

Fig. 10. Comparison between healthy and faulty signals of AN3for 12th IMF

Discrete wavelet decomposition is performed for inspecting the existence of faults in planetary. To detect these faults, sensors AN3 or AN4 are preferred and they have more precise information. Figure 11 shows the comparison between wavelet coefficients of healthy and faulty signals. For the calculation of wavelet decomposition, mother wavelet db4 has been used. According to the figure, there is a peak at the high-speed shaft frequency and a peak at the planetary meshing frequency. Peak amplitude in the faulty signal is higher than the healthy signal and thus fault existence in the planetary gearbox is concluded.

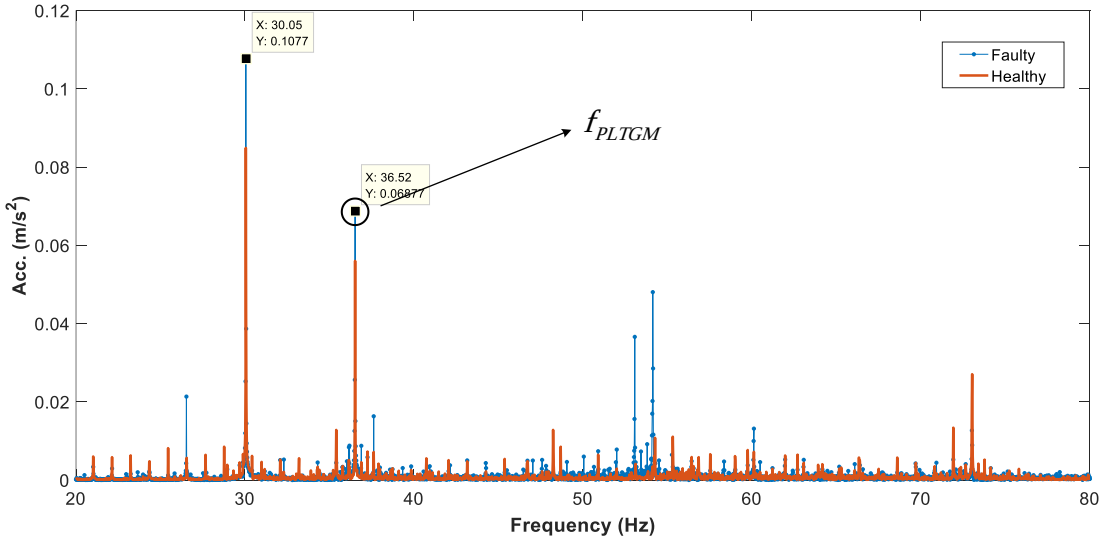

Fig. 11. Comparison of 8th level decomposition of healthy and faulty signals of AN3 in the frequency domain

Table 2. Amplitude factor for 12th IMF of signals and 8th level wavelet coefficient

	Signal 1	Signal 2	Signal 3	Signal 4	Signal 5	Signal 6	Signal 7	Signal 8
NA-MEMD	2.16	2.24	2	1.97	1.92	1.84	1.84	1.83
DWT	1.26	1.31	1.02	1.10	1.09	1.08	1.07	1.08

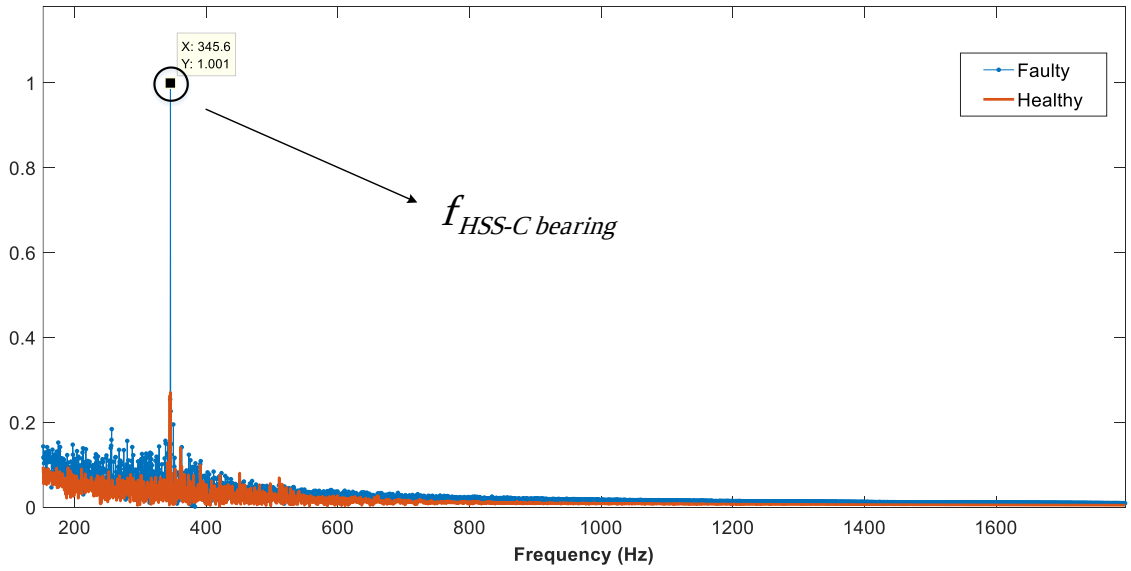

Fig. 12. Comparison between 8th IMF of healthy and faulty signals of AN7

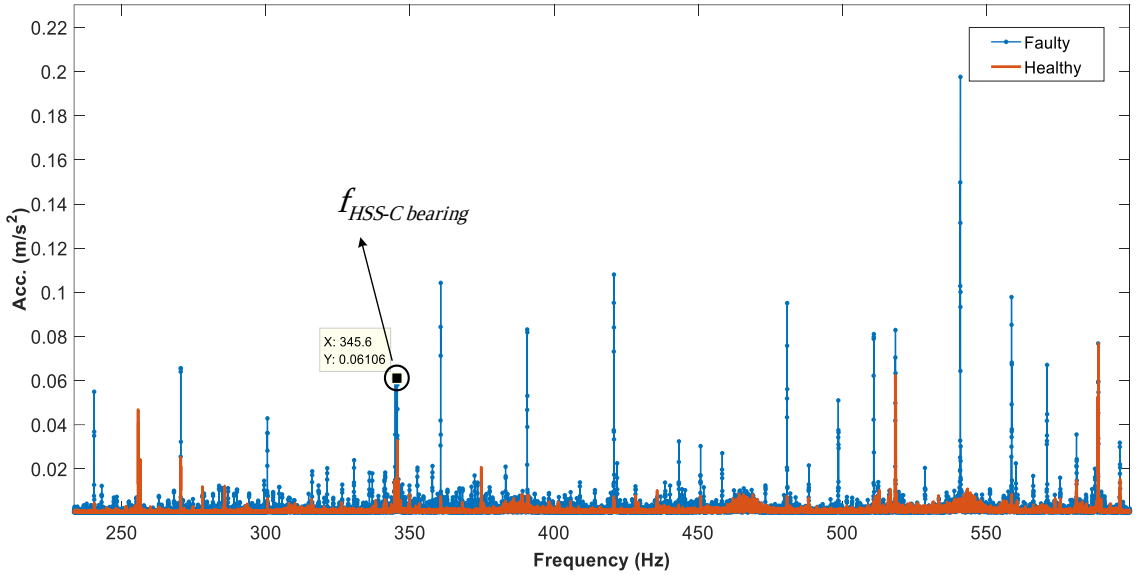

Fig. 13. Comparison of 5th level decomposition of the healthy and faulty signal of AN7 in the frequency domain

Table 3. Amplitude factor for 8th IMF of signals and 5th level wavelet coefficient

	Signal 1	Signal 2	Signal 3	Signal 4	Signal 5	Signal 6	Signal 7	Signal 8
NA-MEMD	3.58	3.67	3.54	3.45	3.7	3.74	3.63	3.63
DWT	1.95	1.98	2.01	2.01	2.23	2.26	2.19	2.17

Table 4. The energy of three different IMFs for sensor signals in healthy conditions

	Signal 1	Signal 2	Signal 3	Signal 4	Signal 5	Signal 6	Signal 7	Signal 8
6th IMF	315.3[a]	304.8	328.9	335	344.4	329.1	333	324
8th IMF	98	91.3	92.6	94	87.9	90.3	97.5	89.8
12th IMF	67.4	69.8	64.5	61.5	61.4	67.4	66.9	64

[a] The energy unit is m^2/s^3 (acceleration^2×time) which is not a physical unit for energy. This energy is divided by impedance so that dimension would be equivalent to physical science.

Table 5. The energy of three different IMFs for sensor signals in faulty conditions

	Signal 1	Signal 2	Signal 3	Signal 4	Signal 5	Signal 6	Signal 7	Signal 8
6th IMF	417.6[a]	405.6	420.1	425.3	421.2	433.2	419.5	418.7
8th IMF	120	133.6	128.8	124.3	127.1	111.5	123.3	124.9
12th IMF	84.5	87.9	89.5	83	81.2	79.6	86.6	90.3

[a] The energy unit is m^2/s^3 (acceleration^2×time) which is not a physical unit for energy. This energy is divided by impedance so that dimension would be equivalent to physical science.

The amplitude factor is used to understand which method can detect faults in planetary gearbox more precisely. The amplitude factor for the 12th IMF and 8th level wavelet coefficient of each of the eight signals are presented in Table 2. According to this table, the amplitude factor for each signal in the MEMD algorithm is higher than the amplitude factor for each signal in the DWT method. So multivariate EMD algorithm can detect faults in the planetary gearbox more precisely and there is more insurance in the existence of a fault in the planetary gearbox by using multivariate EMD.

- High-speed shaft bearing fault

Another dominant fault in this gearbox system is the high-speed shaft bearings fault. Inner race frequency of bearing is $f_{HSS-C\ bearing} = 345.3$ Hz. From Fig. 12, there is a peak at the frequency of 356.6 Hz which is very close to the $f_{HSS-C\ bearing}$. The difference between the amplitude of the peak at this frequency for the healthy and faulty signal is distinguishable (amplitude factor is 3.7). Therefore, according to the multivariate EMD analysis, it can be concluded that the possibility of fault existence at the inner race of HSS-C bearing is high. Fig. 13 shows the comparison between the wavelet coefficient of healthy and faulty signals. There is a peak both in the healthy and faulty signal at the inner race frequency of HSS-C bearing ($f_{HSS-C\ bearing}$). As can be seen, peak amplitude is not as high as previous peaks for other characteristic frequencies. Generally, peak amplitude in bearings is lower than in gears which makes feature extraction more challenging.

Amplitude factors for 8th IMF and 5th level of wavelet coefficient are listed in Table 3. According to this table, amplitude factors for multivariate EMD are higher than DWT. Also, as was mentioned before, the peak amplitude in the wavelet coefficient is low and opposed to IMF peaks. Bearing fault detection is more practical by using than using DWT.

Remark

The concentration of this study is on fault detection of wind turbine gearbox which means locating faults in the system. The energy of IMFs driven from signals can be helpful to just focus on condition monitoring of this system. Comparison between the energy of healthy and faulty IMF leads to perceive if the system is faulty or not and subsequent maintenance actions can be followed afterward. Table 4 shows the energy of three IMFs of each healthy signal and Table 5 is for the faulty one. It should be noted that the energy of the signal is calculated over a band frequency of zero to 20 kHz. By evaluation of these two tables, it can be concluded that there might be a fault in the system, but fault location and characteristics cannot be excluded from these results.

5. Discussion and Conclusion

In this paper, the multivariate empirical mode decomposition algorithm for fault detection of wind turbine planetary gearbox is investigated and also the capability of this algorithm with the discrete wavelet transform is compared. Multivariate EMD is employed to decompose the signals into their intrinsic mode functions. Vibration data is obtained from eight sensors located in different places on the wind turbine gearbox. The high-speed stage, planetary stage, and high-speed shaft bearings are the three gearbox faults. Through numerical and practical applications in the fault detection of wind turbine gearbox and bearings, it has been proved that NA-MEMD outperforms standard EMD algorithm, because both the characteristic frequencies and fault frequencies are extracted from the same IMF groups. This characteristic of the MEMD algorithm can be used to extract fault features automatically. Collecting signals by using multiple sensors from different locations of the gearbox system and the use of multivariate EMD to analyze signals, leads to comprehensive information of all frequency components related to the wind turbine gearbox and bearings. This information is profitable and useful to extract fault features from the system. To remove the influence of input signal noise, NA-MEMD is exploited. In order to have a comparison between NA-MEMD and DWT, the amplitude factor is defined. This factor shows the capability of the NA-MEMD algorithm in detecting fault features in comparison with one of the most common methods of signal processing. In analyzing a signal in the frequency domain, all peaks are not signs of fault in the system and therefore, it must be compared to the healthy condition. By using the amplitude factor criterion, it is concluded that multivariate EMD can extract fault features from the signals more conveniently than discrete wavelet decomposition, especially when dealing with bearing faults, since their peak amplitudes in fault frequencies are not as high as gearbox fault amplitudes. Among the three faults, the high-speed stage fault is more severe, so MEMD and DWT detect this fault precisely. When the system is complex, diagnosis of a specific fault is not easy. For example, planetary stage fault is more

recognizable by using the MEMD algorithm. Bearing fault peak amplitudes are lower in comparison with other faults in the wind turbine gearbox. MEMD has shown its advantage in the diagnosis of bearing faults in this system when the amplitude factor is compared for each method.

Acknowledgments

The authors would like to thank the US Department of Energy (DOE) and the National Renewable Energy Laboratory (NREL) for providing the datasets to support this study.

Funding

This study was not funded by any grant.

Conflict of Interest

The authors declare that they have no conflict of interest.

References

[1] M. Rahnavard, M. Ayati, M. R. Hairi-Yazdi, and M. Mousavi, "Finite time estimation of actuator faults, states, and aerodynamic load of a realistic wind turbine," Renewable Energy, vol. 130, pp. 256-267, January 2019.

[2] S. Zare, and M. Ayati, "Simultaneous fault diagnosis of wind turbine using multichannel convolutional neural network", ISA Transaction, vol. 108, pp.

[3] T. Barszcz, R.B. Randall, Application of spectral kurtosis for detection of a tooth crack in the planetary gear of a wind turbine, Mech. Syst. Signal Process. 23 (2009) 1352–1365. https://doi.org/10.1016/j.ymssp.2008.07.019.

[4] F.P. García Márquez, A.M. Tobias, J.M. Pinar Pérez, M. Papaelias, Condition monitoring of wind turbines: Techniques and methods, Renew. Energy. 46 (2012) 169–178. https://doi.org/10.1016/j.renene.2012.03.003.

[5] M.E. Badaoui, F. Guillet, J. Danière, New applications of the real cepstrum to gear signals, including definition of a robust fault indicator, Mech. Syst. Signal Process. 18 (2004) 1031–1046. https://doi.org/10.1016/j.ymssp.2004.01.005.

[6] J. Antoni, F. Bonnardot, A. Raad, M. El Badaoui, Cyclostationary modeling of rotating machine vibration signals, Mech. Syst. Signal Process. 18 (2004) 1285–1314. https://doi.org/10.1016/S0888-3270(03)00088-8.

[7] L. Satish, Short-time Fourier and wavelet transforms for fault detection in power transformers during impulse tests, IEE Proc. - Sci. Meas. Technol. 145 (1998) 77–84. https://doi.org/10.1049/ip-smt:19981576.

[8] J. LIN, L. QU, Feature extraction based on morlet wavelet and its application for mechanical fault diagnosis, J. Sound Vib. 234 (2000) 135–148. https://doi.org/10.1006/jsvi.2000.2864.

[9] S. Tong, Y. Zhang, J. Xu, F. Cong, Pattern recognition of rolling bearing fault under multiple conditions based on ensemble empirical mode decomposition and singular value decomposition, Proc. Inst. Mech. Eng. Part C J. Mech. Eng. Sci. 0 (2017) 1–17. https://doi.org/10.1177/0954406217715483.

[10] Z.K. Peng, P.W. Tse, F.L. Chu, An improved Hilbert-Huang transform and its application in vibration signal analysis, J. Sound Vib. 286 (2005) 187–205. https://doi.org/10.1016/j.jsv.2004.10.005.

[11] B. Liu, S. Riemenschneider, Y. Xu, Gearbox fault diagnosis using empirical mode decomposition and Hilbert spectrum, Mech. Syst. Signal Process. 20 (2006) 718–734. https://doi.org/10.1016/j.ymssp.2005.02.003.

[12] Y. Yang, D. Yu, J. Cheng, A fault diagnosis approach for roller bearing based on IMF envelope spectrum and SVM, Measurement. 40 (2007) 943–950. https://doi.org/10.1016/j.measurement.2006.10.010.

[13] X. Fan, M.J. Zuo, Gearbox Fault Detection Using Empirical Mode Decomposition, in Nondestruct. Eval. Eng., ASME, 2004: pp. 37–45. https://doi.org/10.1115/IMECE2004-59349.

[14] R. Ricci, P. Pennacchi, Diagnostics of gear faults based on EMD and automatic selection of intrinsic mode functions, Mech. Syst. Signal Process. 25 (2011) 821–838. https://doi.org/10.1016/j.ymssp.2010.10.002.

[15] I. Antoniadou, G. Manson, W.J. Staszewski, T. Barszcz, K. Worden, A time–frequency analysis approach for condition monitoring of a wind turbine gearbox under varying load conditions, Mech. Syst. Signal

Process. 64–65 (2015) 188–216. https://doi.org/10.1016/j.ymssp.2015.03.003.
[16] D.P. Mandic, N. Ur Rehman, Z. Wu, N.E. Huang, Empirical mode decomposition-based time-frequency analysis of multivariate signals: The power of adaptive data analysis, IEEE Signal Process. Mag. 30 (2013) 74–86. https://doi.org/10.1109/MSP.2013.2267931.
[17] D. Looney, D.P. Mandic, Multiscale Image Fusion Using Complex Extensions of EMD, IEEE Trans. Signal Process. 57 (2009) 1626–1630. https://doi.org/10.1109/TSP.2008.2011836.
[18] Y. Lv, R. Yuan, G. Song, Multivariate empirical mode decomposition and its application to fault diagnosis of rolling bearing, Mech. Syst. Signal Process. 81 (2016) 219–234. https://doi.org/10.1016/j.ymssp.2016.03.010.
[19] G. Rilling, P. Flandrin, P. Gonalves, J.M. Lilly, Bivariate Empirical Mode Decomposition, IEEE Signal Process. Lett. 14 (2007) 936–939. https://doi.org/10.1109/LSP.2007.904710.
[20] I. Tsoumas, G. Georgoulas, A. Safacas, G. Vachtsevanos, Empirical Mode Decomposition of the stator start-up current for rotor fault diagnosis in asynchronous machines, in 2008 18th Int. Conf. Electr. Mach., IEEE, 2008: pp. 1–6. https://doi.org/10.1109/ICELMACH.2008.4799987.
[21] N. Rehman, S. Member, D.P. Mandic, S. Member, Empirical Mode Decomposition for Trivariate Signals, IEEE Trans. Signal Process. 58 (2010) 1059–1068. https://doi.org/10.1109/TSP.2009.2033730.
[22] N. Rehman, D.P. Mandic, Multivariate empirical mode decomposition, Proc. R. Soc. A. 466 (2010) 1291–1302. https://doi.org/10.1098/rspa.2009.0502.
[23] X. Zhao, T.H. Patel, M.J. Zuo, Multivariate EMD and full spectrum based condition monitoring for rotating machinery, Mech. Syst. Signal Process. 27 (2012) 712–728. https://doi.org/10.1016/j.ymssp.2011.08.001.
[24] N. Rehman, C. Park, N.E. Huang, D.P. Mandic, EMD Via MEMD: Multivariate Noise-Aided computation of standard EMD, Adv. Adapt. Data Anal. 05 (2013) 1350007. https://doi.org/10.1142/S1793536913500076.
[25] C. Wang, R.X. Gao, R. Yan, Unified time-scale-frequency analysis for machine defect signature extraction: Theoretical framework, Mech. Syst. Signal Process. 23 (2009) 226–235. https://doi.org/10.1016/j.ymssp.2008.03.017.
[26] N.E. Huang, Z. Shen, S.R. Long, M.C. Wu, H.H. Shih, Q. Zheng, N.C. Yen, C.C. Tung, H.H. Liu, The empirical mode decomposition and the Hilbert spectrum for nonlinear and non-stationary time series analysis, Proceeding R. Soc. London. 454 (1998) 903–995. https://doi.org/10.1098/rspa.1998.0193.
[27] Q. Du, S. Yang, Improvement of the EMD method and applications in defect diagnosis of ball bearings, Meas. Sci. Technol. 17 (2006) 2355–2361. https://doi.org/10.1088/0957-0233/17/8/043.
[28] S.G. Mallat, A theory for multiresolution signal decomposition: the wavelet representation, IEEE Trans. Pattern Anal. Mach. Intell. 11 (1989) 674–693. https://doi.org/10.1109/34.192463.
[29] R. Errichello, J.M. Geartech, Gearbox Reliability Collaborative Gearbox 1 Failure Analysis Report December 2010 – January 2011, (2012).